Journal of Materials Chemistry B

PAPER

View Article Online
View Journal | View Issue

Cite this: J. Mater. Chem. B, 2014, 2, 3618

Quantum dot conjugated *S. cerevisiae* as smart nanotoxicity indicators for screening the toxicity of nanomaterials†

Raghuraj S. Chouhan, Anjum Qureshi* and Javed H. Niazi*

Received 28th March 2014
Accepted 3rd April 2014

DOI: 10.1039/c4tb00495g

www.rsc.org/MaterialsB

In this study, we have evaluated the toxicity of different forms of carbon nanotubes (CNTs) using *S. cerevisiae*–QD (SQD) bioconjugates as a novel fluorescent biological nanotoxicity indicator. A CNT mediated effect in SQD bioconjugates was used as an indicator for the changes occurring at the cell–membrane interfaces that induced disruption of membrane bound QDs resulting in the loss of fluorescence. Single, double and multiwalled carbon nanotubes (SWCNTs, DWCNTs and MWCNTs) were tested for their toxicities imposed on SQD bioconjugates. Bioconjugates exposed to varying concentrations of different forms of CNTs exhibited different modes of toxicities on SQD bioconjugates. SQD bioconjugates were highly responsive in the 0.1–10 μg mL^{-1} CNT concentration range after 1 h of exposure. The toxicity of CNTs was linked to the number of CNT walls. These results were further confirmed by SEM analysis and cell-viability tests that were consistent with the toxicity assays using fluorescent bioconjugates with different types of CNTs. SWCNTs imposed more severe cellular toxicity followed by MWCNTs and DWCNTs and the order of increasing cellular-damage by CNTs followed DWCNTs < MWCNTs < SWCNTs. This study speculates that the cell-injury by CNTs depends on their physical properties, such as layers of walls, non-covalent forces and dispersion states. Our results demonstrated a facile optical strategy that enables rapid and real-time cytotoxicity screening with yeast as model living-cells for engineering nanomaterials.

1. Introduction

With the advent of new technologies in the biomedical area, semiconductor quantum dots (QDs) have been successfully used in *in vitro* and *in vivo* imaging,[1,2] immunoassays[3] and FRET based DNA detection.[4] Hence, bioconjugation of QDs is of great importance in biological applications. The carboxylated QDs have been conjugated to the amino groups of biomolecules such as proteins, enzymes, and antibodies.[5] This linking approach is simple and cheap, and currently, it is widely used in certain biosystems. However, QD labeling on whole-cells while keeping the cells alive is scarce, which has great potential for use as whole-cell fluorescence reporters for assessing toxicological impacts on cells.

The use of CNTs in industrial applications and consumer products potentially increases human and environmental exposure.[6] However, CNTs have a number of unique properties which broaden the possible applications in biomedicine.[7] It has been reported that CNTs can be used in cancer therapy;[8] CNTs have been used as nanosyringes[9] and as vehicles for targeted drug delivery.[10] CNTs can exert toxic effects,[11] although this is likely to depend on many factors, including size, type, and concentration of CNTs.[12] Therefore, a more in-depth understanding of the fundamental interactions between CNTs and cell components is required to probe both therapeutic possibilities and potential health risks. The main key element of developing such an understanding is to set apart the interactions of CNTs with cell membranes, especially as both passive penetration and endocytosis have been suggested as mechanisms of internalization.[13] Highly purified pristine SWCNTs exhibit strong antimicrobial activity[14] and the antimicrobial mechanism seems to involve compromised membrane permeability leading to efflux of cytoplasmic material. SWCNTs are significantly more toxic than MWCNTs by effectively damaging the cell membrane.[15]

Recently, several investigators have cautioned that CNTs can interfere with several dye-based cell viability assays.[16–19] Additionally, physical interference due to light absorbance and scattering makes such assays invalid for screening the toxicity of CNTs, Casey *et al.* (2007) have reported that CNTs interact with various dyes commonly used to assess cytotoxicity.[20] Therefore, the studies using the MTT dye based viability assay to report high cytotoxicity of CNTs are now in question. Different

Sabanci University Nanotechnology Research and Application Center, Orta Mah., 34956 Istanbul, Turkey. E-mail: javed@sabanciuniv.edu; anjum@sabaniuniv.edu; Fax: +90 216 483 9885; Tel: +90 216 483 9879

† Electronic supplementary information (ESI) available: Reaction conditions for preparation of bioconjugates; and UV illuminated images of SQD bioconjugates treated with different concentrations of CNTs. See DOI: 10.1039/c4tb00495g

groups have studied the possible physical basis of the interactions of CNTs with membranes by employing molecular dynamics (MD) simulations that showed hydrophobic interactions are the most favored interactions.[21,22]

In our previous work, we studied the effect of MWCNTs on *E. coli*–QD bioconjugates and demonstrated close contact between MWCNTs and bacteria which eventually caused bacterial death.[23] In this work, we have extended further to explore our studies in bioconjugated *S. cerevisiae* yeast cells as a test organism.[24] This species shares major metabolic pathways and homology with humans and advantageous to use as a model organism.[25] We demonstrate that the cytotoxic activity was dependent on the number of walls in CNTs that induced cellular inactivation through piercing, adhesion or wrapping around cell-wall or membrane. All these cytotoxic effects were studied using SQD bioconjugates in which QDs were decorated on cell-surfaces. This enabled determination of the changes in fluorescence intensity with CNT toxicity on cells. The QD-conjugated yeast cells served as an excellent tool to probe responses of living cells to CNT toxicity, which will provide useful information for determining their impact on humans. The current study therefore aimed to investigate the cellular responses with SWCNTs, DWCNTs and MWCNTs on SQD bioconjugates as an initial onset of *in vitro* toxicity.

2. Experimental

2.1. Chemicals, reagents and apparatus

Wild type *S. cerevisiae* (BY-4741) cells were used in the present study to address the toxicological effects of different types of CNTs. Yeast extract, peptone, dextrose broth/agar (YPD) media were purchased from Difco (MI, USA). *N*-Hydroxysuccinimide (NHS), *N*-ethyl-*N*′-(3-(dimethylamino)propyl)carbodiimide (EDC), cysteamine, and tris(2-carboxyethyl)phosphine (TCEP) were purchased from Sigma-Aldrich. SWCNTs (outer diameter, O.D. × length, L = 1–2 nm × 5–20 μm) and MWCNTs (O.D. × L = 10–20 nm × 5–30 μm) were purchased from Arry®, Germany. DWCNTs (O.D. × L = 5 nm × 50 μm) were purchased from Sigma-Aldrich, USA. Triton-X 100 was procured from Merck, Germany. Qdot® 585 and 625 ITK™ carboxyl quantum dots (Invitrogen Co.) were used as labeling probes having emission maxima at 585 and 625 nm, respectively. All other reagents used in this study were of analytical grade and filtered through 0.22 μm sterile filters. CNT samples were dispersed in Triton-X 100 solution (0.01% Triton-X 100 in PBS) and the suspension was ultrasonicated for 15 min using a probe sonicator. A well-dispersed CNT suspension was used as a stock for toxicity studies with SQD bioconjugates.

2.2. Cultivation of *S. cerevisiae* cells

S. cerevisiae cells were freshly grown overnight in YPD-broth at 30 °C and 100 rpm in an orbital shaker and incubated for 20 h. The cells at early stationary phases were harvested by centrifugation at 5000 rpm for 3 min at 4 °C. The cells thus obtained were washed thrice with sterile phosphate buffered saline (PBS, pH 7.4) followed by centrifugation for 5 min at 5000 rpm at 4 °C. The cell pellets were resuspended in the same buffer and colony forming units (CFUs) were determined. Aliquots were made that carried 2×10^9 CFU mL^{-1} for test and control experiments and divided into several sub-aliquots for replicates that carried the same number of cells.

2.3. Covalent linking of QDs on the surface of *S. cerevisiae* using cysteamine and TCEP reduction

In this paper, two different types of QDs were utilized such as QDs having emission at (a) 585 nm appearing bright orange (QD585) and (b) 625 nm appearing intense red color (QD625) for bioconjugation. Coupling of QDs on *S. cerevisiae* cell surfaces was designed to facilitate conjugation to occur on cell-surface disulfide-containing proteins.[26,27] For this, bioconjugation was carried out with cells harvested at the stationary phase that provided sufficient disulfide bridges for coupling using following sequential steps and is schematically shown in Scheme 1.

Step I, covalent coupling of carboxylated QDs with cysteamine was carried out and the reaction mixture contained 8 nM QDs, 8 mM cysteamine, 50 mM EDC and 5 mM NHS in a final volume of 1 mL. This reaction mixture was allowed to stand at RT for 30 min for covalent coupling between –NH_2 of cysteamine and –COOH of carboxyl-QDs. Thus formed cysteamine activated QD suspension was centrifuged at 11 000 rpm for 5 min and the supernatant was discarded. The pellet obtained was resuspended and washed by centrifugation, finally resuspended in PBS, pH 7.4 and stored until use for bioconjugation.

Step II, the *S. cerevisiae* cells (2×10^9 CFU mL^{-1}) were suspended in solution containing 100 μL of 5 mM TCEP and incubated for 20 min at RT to reduce the disulfide bridges of cell-surface membrane proteins. The TCEP treated cells were centrifuged at 5000 rpm for 5 min at 4 °C and washed thrice with PBS (pH 7.4). TCEP was used to reduce the cell-surface disulfide-containing protein motifs to generate free –SH groups in order to facilitate immobilization with cysteamine activated QDs.

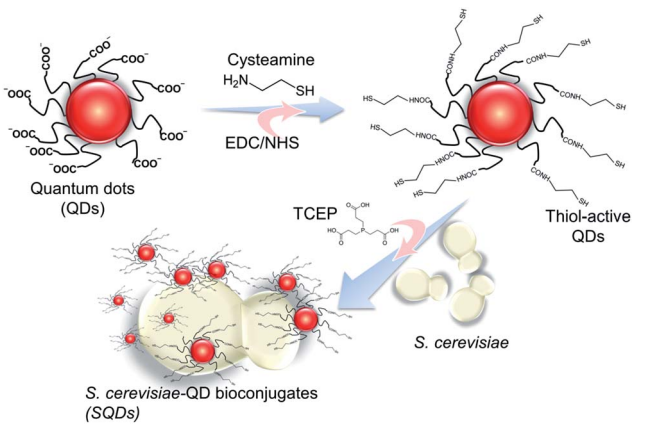

Scheme 1 Schematic diagram of carboxyl-QDs first activating with cysteamine to generate free sulfhydryl groups on QDs using EDC/NHS chemistry. The disulfide linkages on yeast cell-surfaces were then reduced using TCEP to enable formation of disulfide bridges with sulfhydryl activated QDs.

Step III, TCEP treated cells in step II were mixed and incubated for 30 min with SH-activated QDs from step I and the resulting SQDs were centrifuged and washed thrice with PBS, pH 7.4 and stored for further studies. All bioconjugation studies and related work were carried out under sterile conditions.

2.4. Fluorescence measurement

Toxicity studies with different forms of CNTs on SQD bioconjugates were carried using real-time fluorescence scanning at wavelengths ranging from 500–750 nm. The characteristic fluorescent emission peak at 625 nm corresponded to the presence of QDs on cell-surfaces. The fluorescence spectral studies were carried out by using a NanoDrop 3300 Fluorospectrometer (Thermo Scientific NanoDrop Products).

2.5. Treatment of SQDs with different types of CNTs

Different concentrations (0.1, 1 and 10 μg mL^{-1}) of SWCNTs, DWCNTs and MWCNTs in PBS containing 0.01% Triton-X 100 were incubated with SQDs and the fluorescence emission from QDs present on cell-surfaces was recorded initially and after 1 h incubation, keeping the SQD concentration the same in all the aliquots. Any change in the profile of the characteristic peak at 625 nm served as a measure for toxicity assessment against different forms and concentrations of CNTs, respectively. The control samples contained all reaction constituents present in tests except CNTs.

2.6. Confocal microscopic and SEM analysis

Fluorescence microscopy images of SQD bioconjugates were acquired with a Carl-Zeiss LSM 710 confocal microscope equipped with a Plan-Apochromat 63×/1.40 oil objective. QDs on cell-surfaces were excited with a 405 nm laser and images were collected using a 553–718 nm filter. The morphological changes of SQD bioconjugates after incubation with SWCNT, DWCNT and MWCNT suspension solution (10 μg mL^{-1}) were analyzed by using an LEO Supra 35VP Scanning Electron Microscope (SEM). For this SQD bioconjugate treated CNT suspension was dropped on a silica chip and air dried. The fixed samples were sputter coated with gold (10 s, 50 mA) and viewed under the SEM operated at an accelerating voltage (5 keV) depending on the sample type.

2.7. Cell viability of SQD bioconjugates

The cell viability of SQD bioconjugates was first tested and compared with appropriate control after spread plating the diluted cell-suspensions on YPD agar plates. Viable SQD bioconjugates (2×10^9 CFU mL^{-1}) were treated with SWCNTs, DWCNTs and MWCNTs (0.1–10 μg mL^{-1}) and incubated for 1 h at 30 °C. Aliquots of CNT treated SQDs were withdrawn, diluted and spread onto YPD agar plates, respectively and all plates were incubated for 48 h at 30 °C. Untreated SQDs were used as a control and the CFUs were counted to compare with control plates and calculated the survival rates using eqn (1).

$$\text{Survival rate } \% = \frac{\text{number of test CFUs}}{\text{number of control CFUs}} \quad (1)$$

We employed the minimum lethal concentration of all described CNT concentrations taking into account the concentrations used in the literature to assay antimicrobial activity.[28–30]

3. Results and discussion

3.1. Bioconjugation of QDs with *S. cerevisiae*

SQD bioconjugates were prepared by coupling healthy *S. cerevisiae* cells with fluorescent QDs that were designed to serve as nano-switches and turn-off when they interact with CNTs. These SQD bioconjugates were employed to study the cytotoxicity of different forms of CNTs. In this study, to by-pass the effect of internalization, appropriate conjugation chemistry was employed that coupled QDs on yeast cell-wall surfaces and prevented them from internalization. In our previous study, *E. coli* cells were conjugated with QDs using EDC/NHS cross-linking chemistry to study the effects of MWCNTs.[23] In this paper, similar QD bioconjugation attempts using EDC/NHS on yeast cells were unsuccessful. This prompted to a finding that yeast cells have different cell-wall composition and that they require different modes of conjugation. Therefore, carboxyl-QDs were first linked to cysteamine (Cys-SH) using EDC/NHS coupling that yielded free –SH groups on QDs mainly targeting to form bridges with the outer layer disulphide bonds of the yeast cell-wall proteins. Here, TCEP was used to reduce the cell-surface disulfide bridges (from 2×10^9 CFU mL^{-1}) to form free cell-surface –SH groups that were utilized for coupling QD-Cys-SH (Scheme 1) and finally obtained healthy yeast cell–S–S–QD conjugates (SQDs).

QDs have been previously utilized in a variety of live-cell *in vitro* labeling experiments and found no toxicity with such QDs in cultured cells.[31] QDs used in this study were made of a CdSe core encapsulated in a crystalline shell of ZnS and stably coated with an amphophilic polymer which has been designed to prevent the release of free Cd, and therefore QDs in SQD bioconjugates were found to be non-toxic to cells when tested by plating on YPD-agar plates as shown in ESI Fig. S1.† *In vivo* studies carried out by other researchers also confirmed the non-toxic nature of stably protected QDs in mice models.[32,33]

The detailed optimization method and reaction conditions for bioconjugation are shown in ESI Table S1.† The as-prepared SQD bioconjugates were analyzed using confocal microscopy to confirm the uniform labeling of QDs bound on the yeast cell-wall. Fig. 1a–c show the confocal images of QD-bioconjugated yeast cells emitting light at 553–718 nm with confocal laser excitation at 405 nm. The internalization of QDs did not occur as they appear intact as seen in confocal images and the fluorescence emission was seen on the cell-surfaces (Fig. 1a–c). Therefore, the above result indicated that the SQD bioconjugates were stable and retained their cellular integrity upon bioconjugation with water soluble QDs.

The bioconjugates were further examined by SEM analysis to determine any morphological changes that may occur upon bioconjugation with QDs and compared with control cells. As seen in Fig. 2a–c, the SQDs appeared healthy and remained intact upon conjugation with both types of QDs as compared

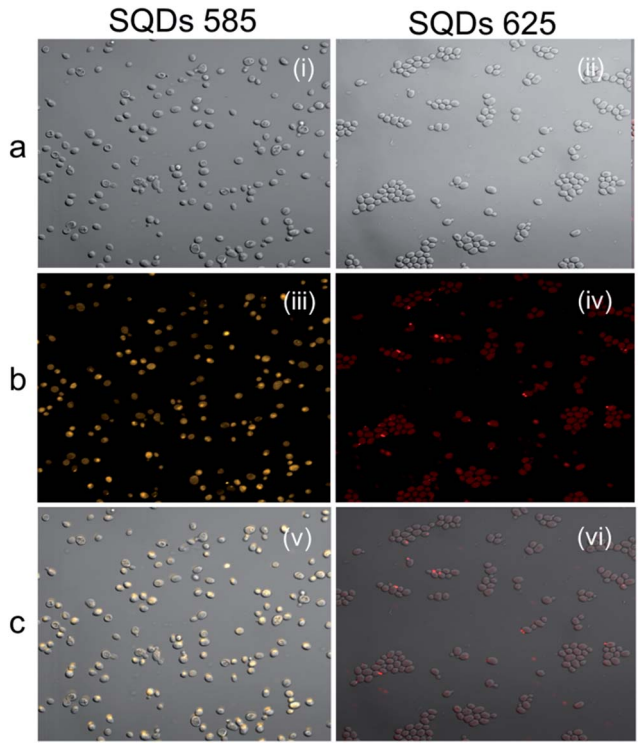

Fig. 1 Confocal images of *S. cerevisiae* (2×10^9 CFU mL^{-1}) coupled with two different types of 8 nM QDs having emission at 585 (left panel) and 625 nm (right panel). Confocal images of the *S. cerevisiae* cells after the incubation with QDs showing (a) bright-field images of SQDs having emission at (i) 585 nm and (ii) 625 nm, (b) fluorescence of QDs excited at 405 nm with (iii) QD585 and (iv) QD625 and (c) overlays of (a and b) with (v) QD585 and (vi) QD625. All images shown in the figure were acquired with a magnification at 40×.

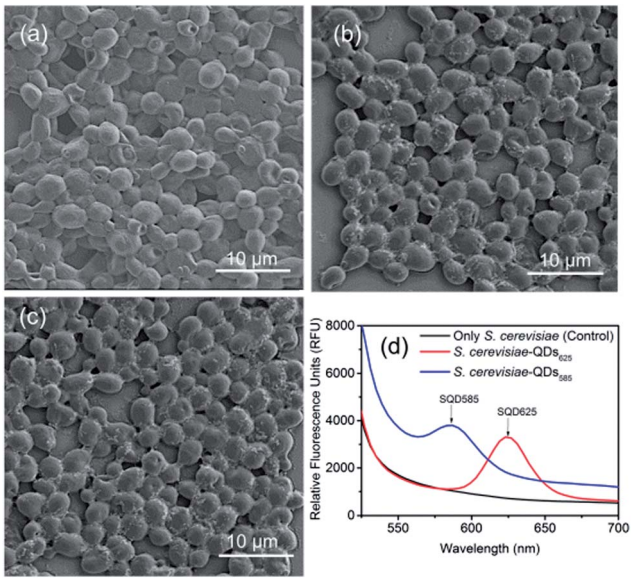

Fig. 2 SEM images and fluorescence spectra of (a) control *S. cerevisiae* cells, (b) SQD bioconjugates containing QDs with emission at 585 nm, (c) SQD bioconjugates containing QDs with emission at 625 nm and (d) fluorescence spectra of control and QD bioconjugated cells. The morphological cellular integrity maintained upon conjugation as cells were smooth and healthy.

with the control. These SQDs were also scanned for their fluorescence emission to ensure that the cell-surface QDs emit fluorescence. The SQD bioconjugate fluorescence scan at 520–700 nm showed distinct characteristic peaks associated with the type of QDs that are highlighted by arrows in Fig. 2d.

SQD bioconjugates with emission at 625 nm were selected for further studies because of their intense red luminescence properties and long-lasting fluorescence responses. To our knowledge, this is the first report on the bioconjugation of yeast cells with SH-QDs using TCEP and S–S cross-linking chemistry. In this study, TCEP was utilized as a reducing agent to anchor –SH activated QDs with the –SH groups of outer cell-surface proteins available on the membrane. The underlying mechanism of QD conjugation on yeast cells can be explained on the basis of the outer cell membrane of *S. cerevisiae*, which mainly consists of mannoproteins with 32–62% of cell-wall disulfide bridges[34,35] that are absent in *E. coli* cells. The outer layer of *S. cerevisiae* heavily contains mannoproteins radiating from the cell surface, which mainly involves in cell recognition and adhesion events.[27] Some proteins on the outer layer are disulphide bonded to other cell wall proteins that are targeted in this study for SH-QD attachment and coupling chemistry. The bioconjugation of QDs on the outer cell surface was achieved also with less impermeable nature of mannoproteins as compared with the inner febrile layer.[27] This is largely due to the presence of carbohydrate side chains and the presence of disulphide bridges. The presence of cell-wall disulphide bridges facilitated the cysteamine coupled QDs with free –SH groups to form –S–S– bridges on cell-walls with TCEP using reduction chemistry. These disulphide linkages have previously been studied and have been used for covalent attachment with various target fusion proteins.[35–37] The harvesting of *S. cerevisiae* cells at the stationary phase for bioconjugation probably provided a maximum number of disulphide bridges (6–7 fold increase) that are available for conjugation with QDs as compared with those cells at lag or log phases.[27]

3.2. SQD bioconjugates as toxic indicators against CNTs

SQD bioconjugates were used as fluorescence indicators for toxicities or cellular damages induced by different types of CNTs (SWCNTs, DWCNTs and MWCNTs) and fluorescence profiles were recorded to probe the onset of toxicity. The extent of toxicity with various concentrations of CNTs (0.1–10 μg mL^{-1}) was studied through changes in SQD bioconjugates' fluorescence emission characteristics. Fig. 3a–c show the fluorescence emission levels with the influence of the number of walls present in CNTs. The disintegration of fluorescence emission is postulated to have occurred due to physical perturbations of CNTs on cell-surfaces and associated QD de-localization at the cellular interfaces. SWCNTs exhibited severe cellular damage followed by MWCNTs, therefore causing a significant drop in fluorescence emissions from SQDs. Interestingly, DWCNTs were found to be relatively less toxic compared with SWCNTs or MWCNTs. At a higher 10 μg mL^{-1} concentration, SW/MWCNTs

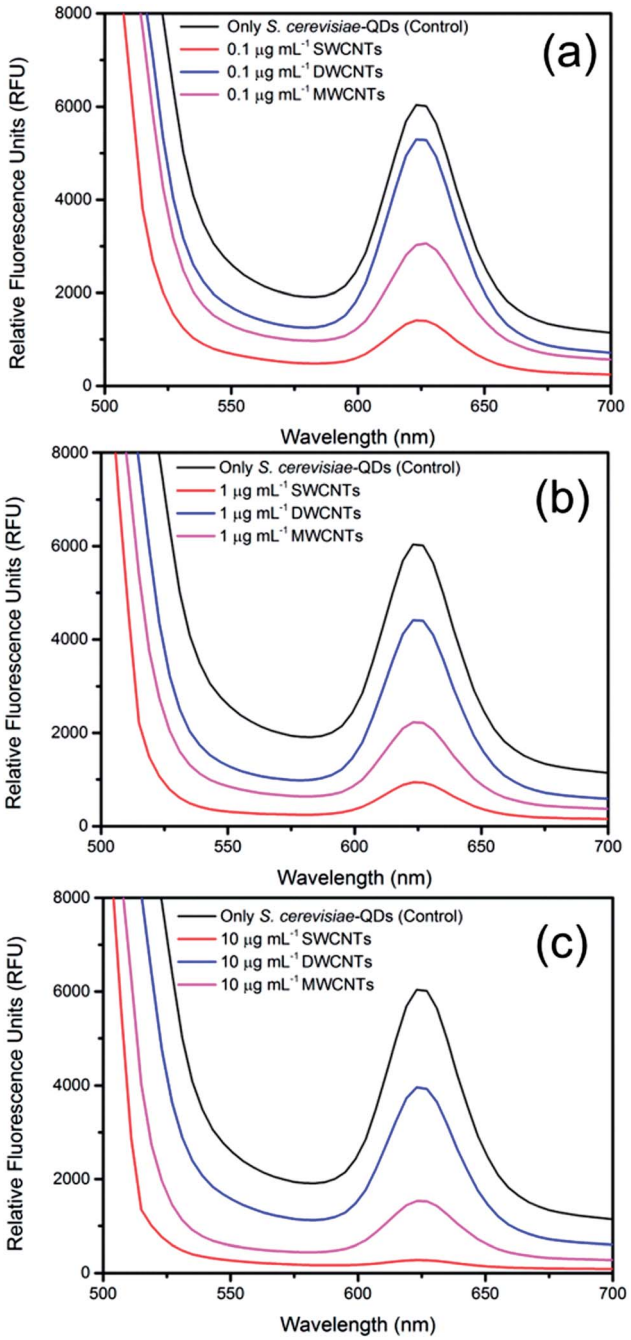

Fig. 3 Fluorescence emission spectra of SQD bioconjugates after interaction with homogeneous suspension of (a) 0.1, (b) 1.0 and (c) 10 μg mL^{-1} concentrations of SWCNTs, DWCNTs and MWCNTs.

exhibited significant loss of fluorescence associated with QDs on cell surfaces (Fig. 4a) which was evidenced by a drastic loss of fluorescence emission at 625 nm compared to the control or DWCNT treated SQD bioconjugates.

RFU responses with SQD bioconjugates were correlated with the number of cells that survived after their interaction with CNTs (CFU mL^{-1}) (Fig. 4b). A significantly higher toxicity with SWCNTs occurred which can be attributed to their physico-chemical properties, higher surface area and shorter length compared to those of MWCNTs exhibiting a greater extent of interaction at the outer cell membranes.[15] Cell viability assays using SQD bioconjugates were carried out to monitor the effect of CNTs on cell-viability to examine the number of cells survived after the treatment with 0.1, 1 and 10 μg mL^{-1} single, double and multi-walled CNTs for 1 h (Fig. 4b). At maximum 10 μg mL^{-1}, about 50% of cells survived with DWCNT exposure. In contrast, 75% reduction in the CFUs occurred with MWCNT treated samples. SWCNTs however showed the highest activity inducing 90% CFU reduction. As with the lower 0.1–1 μg mL^{-1} concentrations, SWCNTs seem to significantly inhibit the cell growth as compared with DWCNTs and MWCNTs (Fig. 4a and b). The above results strongly suggested that the damage to the cell envelope was an initial effect that, in turn, caused proportional reduction in the number of CFUs. Hence, a different CNT-to-yeast cell interaction likely to occur compared to bacteria, and this could be accounted for by a completely different cell-wall chemistry and structure.[38]

3.3. Morphological changes and cell viability

SEM images of SQD bioconjugates were taken in their native forms and after incubation with SWCNTs, DWCNTs and MWCNTs (10 μg mL^{-1}) for 1 h (Fig. 5a–d). Morphological changes occurred in the cells with the interaction of CNTs revealed deformation and loss of cellular integrity with SWCNTs and MWCNTs (Fig. 5b and d). In contrast, cells exposed to DWCNTs maintain the cellular integrity with the majority of cells still intact with their membrane structure (Fig. 5c). All three types of CNTs were able to interact or damage the cell membrane through the means of piercing or adhesion or wrapping depending upon the number of CNT-walls. We observed a strong correlation between fluorescent spectra, cell-viability and morphological pattern change by SEM analysis that demonstrated toxic effects of SWCNTs, and MWCNTs followed by mild toxic effects with DWCNTs on SQD bioconjugates (Fig. 4a and b and 5a–d). The nanosize, shape and high aspect ratios of CNTs allow their penetration through the membrane, which has been experimentally studied.[39] A similar type of mechanism was also observed with all forms of CNTs towards SQD bioconjugates.

Morphological changes by examining the SEM images of SQD bioconjugates' interaction with CNTs displayed concentration and type dependent toxicities in yeast. CNTs were found to make direct contact with yeast cell-wall *via* piercing, adhesion and wrapping. The outermost region of the cells is the most accessible layer for interaction with many drugs and particulate matter, therefore yeast structural integrity is vital for survival.[38] Here, puncturing of the cell-wall occurred predominantly by SWCNTs and similar indications were observed for MWCNTs (Fig. 5b and d). However, no such detrimental effects were noticed with DWCNTs (Fig. 5c). The characteristic features of different numbers of CNT-walls probably have influenced the survival rates of cells which likely depend on the physico-chemical and unique structural properties of CNTs.[40] Based on the above results, possible mechanisms by which yeast cells interacted with different forms of CNTs are schematically shown in Scheme 2.

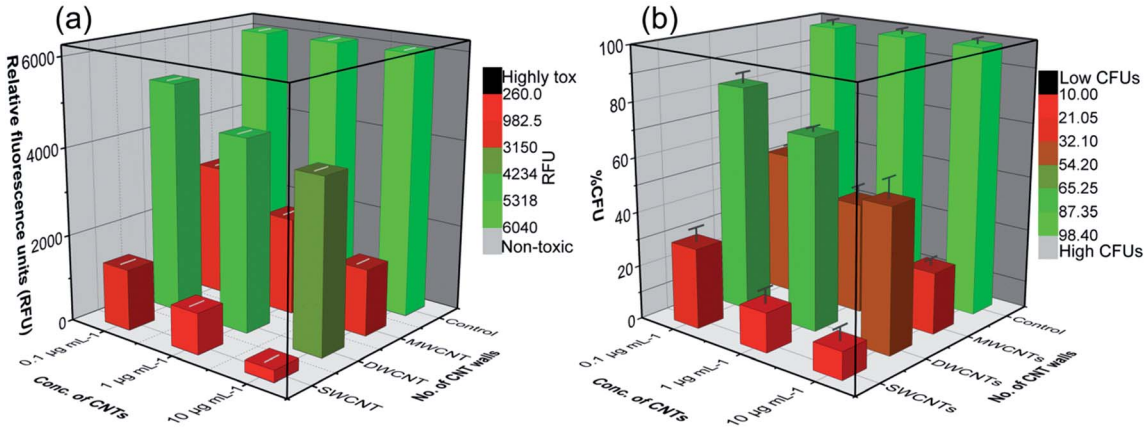

Fig. 4 3D bar plots of bioconjugates: (a) RFU responses against different types and concentrations of CNTs extracted from the spectral data from emissions at 625 nm for comparison, and (b) corresponding surviving number of cells (CFU mL^{-1}). The color maps in (a) and (b) indicate toxicity index in which color red represents severe cellular damage and green indicates unaffected or less-toxic effects.

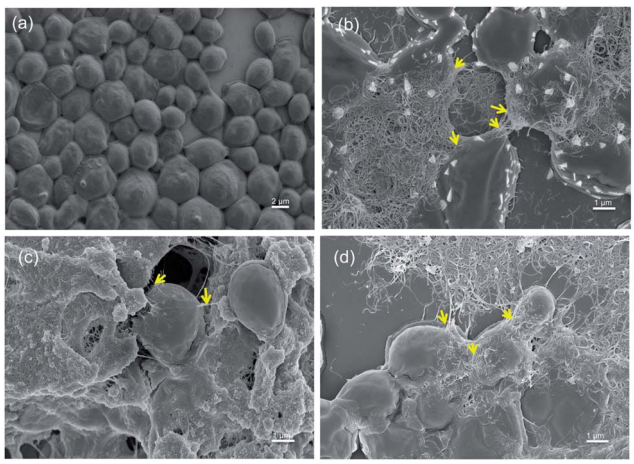

Fig. 5 SEM images of SQD bioconjugates before control (a) and after the treatment with SWCNTs (b), DWCNTs (c), and MWCNTs (d) suspensions at a concentration of 10 μg mL^{-1}. The arrows indicate the cell–CNT interfaces and the location of damage occurring in SQD bioconjugates (yeast cells).

Interestingly, it was observed in this study that MWCNTs wrapped around the surface of yeast cells which potentially induce osmotic shock in cells.[41] DWCNTs act as a scaffold enhancer similar to the reports of graphene oxide materials, which tended to produce a dramatic increase in cell adhesion or attachment.[42] Thus, the type of CNTs is a critical factor in antifungal activity, which is dependent on the number of CNT-walls interacting on the cell surface.

We hypothesize that in addition to the physical piercing, adhesion and wrapping mechanisms, the size and type of CNTs may facilitate chemical interactions, such as hydrogen-bonding or electrostatic absorption with the microbial cell-wall, thus disintegrating the cell-wall/membrane and eventually leading to cell death. The primary interactions of cells with external perturbations, such as in this case CNTs, first occur at the 'interface of the cell surface and the external environment' to cause biological toxicity. Therefore, primary interactions with different forms of CNTs on *S. cerevisiae* cells appeared to have taken place at the cell-wall interfaces, where QDs are harbored (SQDs). The cell-bound QDs therefore served as nano-switches because of their efficient fluorescence switching-off mechanism upon interaction with CNTs, because of their detrimental effects on cell-bound QDs. The events of cellular damage were examined through visualizing or measuring the residual fluorescence (spectral analysis) from the CNT-treated SQD bioconjugates. Here, the tubes containing the reaction mixture were subjected to a rapid toxicity screening assay for qualitative analysis by simply exposing the reaction tubes under UV light (see ESI Fig. S2a–c†). Qualitative (Yes/No) tests were carried out to assess rapid visible changes of the above effects with SQD bioconjugates exposed to SWCNTs, DWCNTs and MWCNTs. Thus, exposure of bioconjugates to CNTs is postulated to promote the loss of fluorescence as a result of cellular stress,

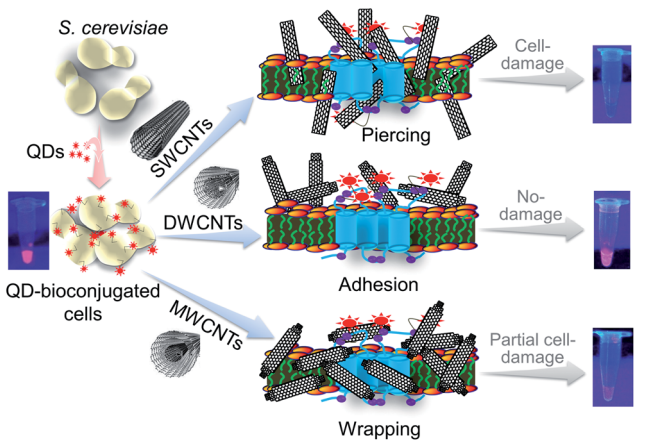

Scheme 2 Possible underlying mechanisms of interaction of SWCNTs, DWCNTs and MWCNTs on SQD bioconjugates (yeast cells). The tubes showing the fluorescence emissions originating from QDs present on yeast-cell surfaces after exciting briefly under UV light. The disintegrating fluorescence emission from the tubes is the indication of cellular damage or disruption of cells.

either through the deformation of the outer cellular surface or damage to the cells. Comparative response patterns of SQD bioconjugates in fluorescence emission with single and multi-walled CNTs consistently revealed their harmful effects on the integrity of *S. cerevisiae* cells. It is clear that more severe the toxicity, more rapidly the fluorescence disintegrated from SQD bioconjugates, which can be related to the loss of cellular integrity (see ESI Fig. S2b–c†). This result indicated that the contact of yeast cells with CNTs depended on either the single or the multi-walled nature of CNTs to irreversibly damage the cell-membrane integrity and thus damaged the cells leading to disruption of the membrane bound QDs.[23] However, results with DWCNTs appeared to have induced relatively low toxicity which is probably due to the adhesion but not piercing or wrapping mechanism seen in SWCNTs or MWCNTs, respectively as schematically illustrated in Scheme 2.

Many conventional antibiotics interact with specific target molecules within the microbes causing double-stranded DNA breakage, disturbance of protein synthesis and blocking of cell division.[43] As a result, the morphology of the cell is preserved and, consequently, the cell can easily develop resistance. Therefore, an antibacterial/fungal agent, such as modified CNTs that may have specific ability to interact against multi-drug-resistant microbes, is urgently required. CNTs can be functionalized in a way that they specifically targeted to interact with pathogenic microbes. Such targeted CNTs can physically damage the cell-walls or membranes of drug-resistant microbes.

The present work shows that different forms of CNTs may be toxic to microbes during their application or exposure, suggesting a potential risk to human health. However, in light of their cytotoxic activity, functionalized CNTs directed toward their specific interacting with pathogens display a potential biomedical application as effective, selective, and broad-spectrum antibacterial/fungal agents, especially meaningful in the treatment of drug-resistant microbes. With this kind of analysis we cannot ascertain how deeply the CNT bundles enter inside the cells. We conclude that they reach at least the cell membrane and that the subsequent interactions between the CNT chemical surface groups and the cell constituents affect the intracellular redox balance, as supported by the decreased fluorescence signals.

4. Conclusions

CNTs find valuable applications in the environment, and in manufacturing and biomedical sectors as well as food and agriculture industries. There has been a recent focus on how specific physicochemical properties of CNTs influence cytotoxicity. The ultimate goal is to understand the relationship between the fundamental physicochemical properties of CNTs and the cytotoxic mechanism in order to both advance functional design and to minimize unintended consequences of CNTs. Quantum dot (QD) decorated living-cell conjugates with optical interfaces possess unique properties that are most desirable in biomedical and environmental applications. Here we have reported that SWCNTs, DWCNTs and MWCNTs possess different modes of antifungal activity towards *S. cerevisiae* cells. These effects could not be correlated with any specific CNT chemical–physical characteristics but could be ascribed to the ability of CNT networks to attract and capture pathogens through van der Waals forces with respect to single, double and multi-walled CNTs. Moreover, to investigate whether CNTs could affect the cell membrane integrity towards *S. cerevisiae* cells, we conjugated the cells with QDs and used as toxic indicators. Though the cell-wall composition is far different from bacteria, TCEP cross-linking chemistry was utilized in the present work. Our finding supported the hypothesis that a piercing, adhesion and wrapping effect with SWCNTs, DWCNTs and MWCNTs, respectively, could be responsible for the observed reduced capacity of forming colonies by the cells. Here, the order of increasing toxicity in yeast cells followed DWCNTs < MWCNTs < SWCNTs. Our investigation highlights that CNTs possess different antifungal properties not clearly related to CNTs' specific characteristics, but to the direct interaction with the microbial pathogen wall, which needs further investigation. At extreme conditions, such as with high levels of CNTs, the SQD bioconjugates tend to lose surface QDs due to partial/complete dispersion of cell-bound QDs consistent with the loss of cell-viability. SWCNTs, DWCNTs and MWCNTs used in this study alone exhibited no significant quenching with free QDs. It exemplifies that quenching of QDs on bioconjugates may not have taken place, or cellular enzymes released in response to CNTs following collapse of cell-structure may be responsible for partial quenching of QDs on bioconjugates. Changes due to cytotoxicity in bioconjugates can be visually observed by illuminating the SQDs with the UV-light and thus enabling rapid and robust toxicity screening for a large number of samples. These results confirm that CNTs possess the intrinsic potential to act as an antifungal tool that could be exploited in biomedical devices and/or in filtering systems for hospital and industrial cleaning applications.

Acknowledgements

This work was supported by the Scientific and Technological Research Council of Turkey (TUBITAK), project grant nos 112Y309 and 112E051 for JHN and AQ, respectively. We thank Dr H. Unal for her assistance with confocal microscopy.

Notes and references

1 P. K. Bae, K. N. Kim, S. J. Lee, H. J. Chang, C. K. Lee and J. K. Park, *Biomaterials*, 2009, **30**, 836–842.
2 Y. He, Y. Y. Su, X. B. Yang, Z. H. Kang, T. T. Xu, R. Q. Zhang, C. H. Fan and S. T. Lee, *J. Am. Chem. Soc.*, 2009, **131**, 4434–4438.
3 J. V. Jokerst, A. Raamanathan, N. Christodoulides, P. N. Floriano, A. A. Pollard, G. W. Simmons, J. Wong, C. Gage, W. B. Furmaga, S. W. Redding and J. T. McDevitt, *Biosens. Bioelectron.*, 2009, **24**, 3622–3629.
4 C. S. Wu, J. M. Cupps and X. D. Fan, *Nanotechnology*, 2009, **20**(5), 305502.

5 I. L. Medintz, E. R. Goldman, M. E. Lassman and J. M. Mauro, *Bioconjugate Chem.*, 2003, **14**, 909–918.
6 B. Nowack, R. M. David, H. Fissan, H. Morris, J. A. Shatkin, M. Stintz, R. Zepp and D. Brouwer, *Environ. Int.*, 2013, **59**, 1–11.
7 K. Kostarelos, A. Bianco and M. Prato, *Nat. Nanotechnol.*, 2009, **4**, 627–633.
8 N. W. S. Kam, M. O'Connell, J. A. Wisdom and H. J. Dai, *Proc. Natl. Acad. Sci. U. S. A.*, 2005, **102**, 11600–11605.
9 X. Chen, A. Kis, A. Zettl and C. R. Bertozzi, *Proc. Natl. Acad. Sci. U. S. A.*, 2007, **104**, 8218–8222.
10 Z. D. Su, S. H. Zhu, A. D. Donkor, C. Tzoganakis and J. F. Honek, *J. Am. Chem. Soc.*, 2011, **133**, 6874–6877.
11 C. A. Poland, R. Duffin, I. Kinloch, A. Maynard, W. A. H. Wallace, A. Seaton, V. Stone, S. Brown, W. MacNee and K. Donaldson, *Nat. Nanotechnol.*, 2008, **3**, 423–428.
12 K. Kostarelos, *Nat. Biotechnol.*, 2008, **26**, 774–776.
13 C. P. Firme and P. R. Bandaru, *J. Nanomed. Nanotechnol.*, 2010, **6**, 245–256.
14 C. N. Yang, J. Mamouni, Y. A. Tang and L. J. Yang, *Langmuir*, 2010, **26**, 16013–16019.
15 S. Kang, M. Herzberg, D. F. Rodrigues and M. Elimelech, *Langmuir*, 2008, **24**, 6409–6413.
16 N. A. Monteiro-Riviere and A. O. Inman, *Carbon*, 2006, **44**, 1070–1078.
17 J. M. Worle-Knirsch, K. Pulskamp and H. F. Krug, *Nano Lett.*, 2006, **6**, 1261–1268.
18 M. Davoren, E. Herzog, A. Casey, B. Cottineau, G. Chambers, H. J. Byrne and F. M. Lyng, *Toxicol. in Vitro*, 2007, **21**, 438–448.
19 K. Pulskamp, J. M. Worle-Knirsch, F. Hennrich, K. Kern and H. F. Krug, *Carbon*, 2007, **45**, 2241–2249.
20 A. Casey, E. Herzog, M. Davoren, F. M. Lyng, H. J. Byrne and G. Chambers, *Carbon*, 2007, **45**, 1425–1432.
21 E. J. Wallace and M. S. P. Sansom, *Nano Lett.*, 2007, **7**, 1923–1928.
22 A. J. Makarucha, N. Todorova and I. Yarovsky, *Eur. Biophys. J.*, 2011, **40**, 103–115.
23 R. S. Chouhan, J. H. Niazi and A. Qureshi, *J. Mater. Chem. B*, 2013, **1**, 2724–2730.
24 K. Kasemets, A. Ivask, H. C. Dubourguier and A. Kahru, *Toxicol. in Vitro*, 2009, **23**, 1116–1122.
25 S. Grossetete, B. Labedan and O. Lespinet, *BMC Genomics*, 2010, **11**, 81.
26 Y. Yang, Y. L. Song and J. Loscalzo, *Proc. Natl. Acad. Sci. U. S. A.*, 2009, **106**, 14734.
27 Y. Yang, Y. Song and J. Loscalzo, *Proc. Natl. Acad. Sci. U. S. A.*, 2007, **104**, 10813–10817.
28 R. N. Su, Y. J. Jin, Y. Liu, M. P. Tong and H. Kim, *Colloids Surf., B*, 2013, **104**, 133–139.
29 X. P. Wang, X. Q. Liu and H. Y. Han, *Colloids Surf., B*, 2013, **103**, 136–142.
30 T. Akasaka, M. Matsuoka, T. Hashimoto, S. Abe, M. Uo and F. Watari, *Mater. Sci. Eng., B*, 2010, **173**, 187–190.
31 J. K. Jaiswal, H. Mattoussi, J. M. Mauro and S. M. Simon, *Nat. Biotechnol.*, 2003, **21**, 47–51.
32 B. Ballou, B. C. Lagerholm, L. A. Ernst, M. P. Bruchez and A. S. Waggoner, *Bioconjugate Chem.*, 2004, **15**, 79–86.
33 H. Ding, K. T. Yong, W. C. Law, I. Roy, R. Hu, F. Wu, W. Zhao, K. Huang, F. Erogbogbo, E. J. Bergey and P. N. Prasad, *Nanoscale*, 2011, **3**, 1813–1822.
34 F. M. Klis, M. de Jong, S. Brul and P. W. J. de Groot, *Yeast*, 2007, **24**, 253–258.
35 J. G. Denobel, F. M. Klis, J. Priem, T. Munnik and H. Vandenende, *Yeast*, 1990, **6**, 491–499.
36 Y. Shibasaki, N. Kamasawa, S. Shibasaki, W. Zou, T. Murai, M. Ueda, A. Tanaka and M. Osumi, *FEMS Microbiol. Lett.*, 2000, **192**, 243–248.
37 K. Hamada, H. Terashima, M. Arisawa, N. Yabuki and K. Kitada, *J. Bacteriol.*, 1999, **181**, 3886–3889.
38 M. Olivi, E. Zanni, G. De Bellis, C. Talora, M. S. Sarto, C. Palleschi, E. Flahaut, M. Monthioux, S. Rapino, D. Uccelletti and S. Fiorito, *Nanoscale*, 2013, **5**, 9023–9029.
39 D. Pantarotto, R. Singh, D. McCarthy, M. Erhardt, J. P. Briand, M. Prato, K. Kostarelos and A. Bianco, *Angew. Chem., Int. Ed.*, 2004, **43**, 5242–5246.
40 C. D. Vecitis, K. R. Zodrow, S. Kang and M. Elimelech, *ACS Nano*, 2010, **4**, 5471–5479.
41 H. Q. Chen, B. Wang, D. Gao, M. Guan, L. N. Zheng, H. Ouyang, Z. F. Chai, Y. L. Zhao and W. Y. Feng, *Small*, 2013, **9**, 2735–2746.
42 O. N. Ruiz, K. A. S. Fernando, B. J. Wang, N. A. Brown, P. G. Luo, N. D. McNamara, M. Vangsness, Y. P. Sun and C. E. Bunker, *ACS Nano*, 2011, **5**, 8100–8107.
43 F. Nederberg, Y. Zhang, J. P. K. Tan, K. J. Xu, H. Y. Wang, C. Yang, S. J. Gao, X. D. Guo, K. Fukushima, L. J. Li, J. L. Hedrick and Y. Y. Yang, *Nat. Chem.*, 2011, **3**, 409–414.